JOURNAL OF MATERIALS SCIENCE 28 (1993) 5045–5049

Investigation of the crystal growth of CuO from the $CuO–Bi_2O_3$ system

CHEN CHANGKANG, HU YONGLE, B. M. WANKLYN, J. W. HODBY, F. R. WONDRE
Clarendon Laboratory, University of Oxford, Parks Road, Oxford OX1 3PH UK

The relationship between properties and structure in high-temperature superconducting copper oxides has stimulated the investigation on the properties of single crystal CuO. The phase diagram of $CuO–CuBi_2O_4$ has been established by improved thermogravimetric analysis (ITGA), differential thermal analysis (DTA) and X-ray diffraction. The crystallization temperature of CuO was determined by ITGA and the dependence of crystallization temperature on cooling rates showed about 20 °C supercooling in the crystal growth of CuO from the $CuO–Bi_2O_3$ system. Using the theory of crystal growth under stable state conditions, an initial kinetic analysis of seed crystal dissolution was also performed on the ITGA data. Using the phase diagram and the ITGA information, large crystals have been grown near the surface of the high-temperature solution or the bottom of the crucible by a combination of ITGA and the top-seeding method.

1. Introduction

CuO belongs to the monoclinic space group, C2/c, $Z = 4$ [1]. Each copper atom is nearly rectangularly coordinated by four oxygen atoms forming a CuO_4 plate, in which the copper–oxygen interaction is similar to that at the Cu (2) site of $YBa_2Cu_3O_{7-y}$. Ribbons of side-sharing (CuO_4) plates extend along the [1 1 0] direction. In addition, each oxygen atom is enclosed in a tetrahedron of copper atoms, generating further ribbons along $[1\bar{1}0]$. Although CuO is an insulating material, the interest in the relationship between the physical properties and the structure of the high T_c cuprate materials has stimulated many studies on single-crystal CuO, such as magnetism [2], electric field gradient [3] and neutron diffraction [4].

CuO is subject to incongruent melting with loss of oxygen at 1026 °C in air [5]

$$CuO \rightarrow Cu_2O + 1/2\,O_2 \quad (1)$$

Single crystals of CuO, therefore, have to be grown by the flux method. KF [6], $PbCl_2 + PbF_2$ [7] and $MoO_3 + V_2O_5 + K_2CO_3$ [8] have previously been used as the flux, producing small or long dendritic crystals. Recently, we have studied the application of BaO and of Bi_2O_3 as flux to grow CuO crystals. As is well known, BaO and Bi_2O_3 are common components of the high T_c superconducting materials and the most useful self-flux for crystal growth of the superconducting Y–Ba–Cu–O, Bi–Sr–Ca–Cu–O and $BaPb_{1-x}Bi_xO_3$ families. A study of the CuO–BaO and $CuO–Bi_2O_3$ systems will be of assistance in understanding the crystal growth not only of CuO, but also of the related superconducting materials. The phase diagram and crystal growth of CuO from BaO flux have been reported elsewhere [9]. Here, some results of a physico-chemical investigation of the crystal growth of CuO from the $CuO–Bi_2O_3$ system are described.

A phase diagram of $CuO–Bi_2O_3$ was published in 1966 [10], which showed only one compound, $CuBi_4O_7$, to exist in the system. After initial studies of crystal growth, we thought it necessary to establish the CuO-rich part of the phase diagram by differential thermal analysis (DTA) and improved thermogravimetric analysis (ITGA). Used *in situ* for crystal growth, ITGA can provide important information on crystal growth, including the crystallization temperature and kinetic analysis of crystal growth, crystal dissolution and flux evaporation. It has also been applied in physico-chemical research of the crystal growth of various superconducting materials [11–16]. After determination of the crystallization temperature, crystal growth is initiated by introducing a seed crystal or a wire as the nucleation centre. The process of crystal growth is traced by the thermogravimetric curve and is terminated by lifting the crystal out of the solution above the eutectic temperature.

2. Experimental procedure

The chemicals were BDH Laboratory Reagent Grade 99% Bi_2O_3 and BDH "Analar" 98% CuO. Two furnaces with electrical balances were used for ITGA and crystal growth. One was a vertical tube furnace with an SiC spiral heating element, whose temperature was regulated by a Eurotherm controller combined with a digital programmer made in Clarendon Laboratory. The other one was a three-zone tube furnace wound by Pt–Rh wires. The zone temperatures were separately controlled by Eurotherm 818 controller-programmers. Pt–PtRh thermocouples were used to control and measure the temperature. Alumina or platinum crucibles were used. After a long period of crystal growth, the alumina crucible was seriously attacked,

0022–2461

showing the platinum crucible to be more suitable for the CuO–Bi_2O_3 system. For improved thermogravimetric analysis, a platinum wire or seed was immersed into the high-temperature solution to act as the nucleation or growth centre, and a curve showing the apparent weight was recorded by a chart recorder. A thermocouple underneath the crucible was used to measure the temperature. For the phase diagram, the eutectic temperature was determined by DTA in an alumina crucible heated at $10\,^{\circ}C\,min^{-1}$ in air. The thermal effect of the liquidus line was too small to be detected by DTA. ITGA was therefore utilized for determination of the liquidus line and the crystalline phase was identified by X-ray diffraction. An 80 g mixture with starting composition of $CuO:Bi_2O_3 = 1:1$ (mol) was charged in an alumina crucible. After measuring the crystallization temperature by ITGA using a platinum wire as a probe under a cooling rate of $200\,^{\circ}C\,h^{-1}$ in air, a certain amount of CuO was added to the system. After holding at high temperature for 20 h to form a completely dissolved and homogeneous solution, measurement was again performed. In this way the liquidus line was obtained in the range between 50 and 73.3 mol % CuO. Meanwhile, the crystallization temperature was measured at different cooling rates or by a seed crystal in the solution with the same concentration. The dissolution of a seed crystal was also recorded at a constant temperature with superheating.

3. Results and discussion

3.1. CuO–$CuBi_2O_4$ phase diagram

According to the published diagram of CuO–Bi_2O_3 [10], we first chose the starting composition of $0.43CuO$–$0.57Bi_2O_3$ to grow CuO crystals. No CuO crystal was obtained. Instead we found crystals of $CuBi_2O_4$, which were not shown in the phase diagram. Fig. 1 shows the X-ray diffraction powder pattern of $CuBi_2O_4$. It was therefore necessary to establish a new phase diagram by ITGA and DTA experiments.

Fig. 2 shows the phase diagram of CuO–$CuBi_2O_4$. X-ray diffraction showed that the crystalline phase grown from the starting composition of $CuO:Bi_2O_3 = 0.5:0.5$ (mol) is $CuBi_2O_4$. If the ratio of $CuO:Bi_2O_3$ was higher than 0.53:0.47 (mol), the crystalline phase was CuO. The phase diagram is a typical eutectic system, in which the eutectic temperature is around 845 °C and the eutectic composition is located in $CuO:Bi_2O_3 = 0.53:0.47$ (mol). A wide liquidus range exists for crystal growth of CuO, and the liquidus line represents the solubility of CuO in the flux system. Fig. 3 shows that the solubility, S, at various temperatures T follows the Arrhenius expression

$$S = S_0 \exp(-H/RT) \qquad (2)$$

in which H is the heat of crystallization of CuO in the system, which is determined to be 52.1 kcal mol^{-1} by the method of least squares, and R is the gas constant.

3.2. Crystallization temperature

In Fig. 4 a typical ITGA curve shows the crystallization and dissolution of CuO on an immersed platinum wire in the flux system Bi_2O_3–CuO. Above the crystallization temperature, the whole system was completely

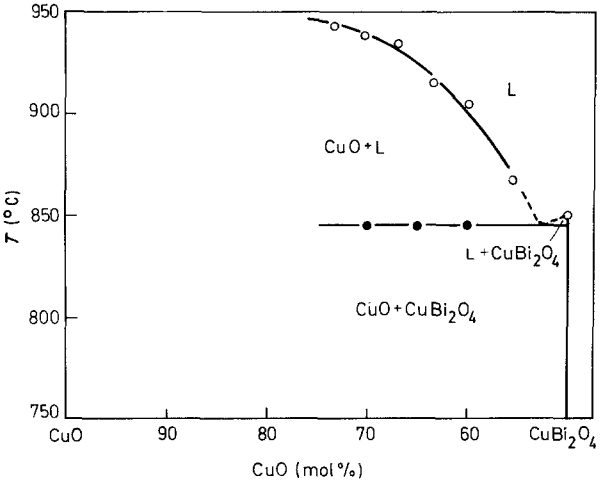

Figure 2 The phase diagram of the CuO–$CuBi_2O_4$ system. (○) ITGA, $200\,^{\circ}C\,h^{-1}$; (●) DTA $600\,^{\circ}C\,h^{-1}$.

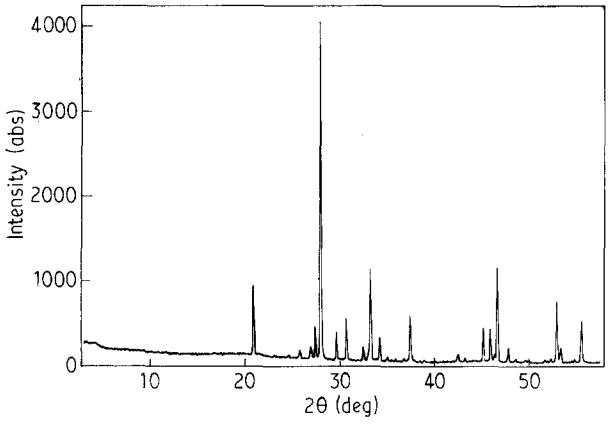

Figure 1 X-ray diffraction powder pattern of $CuBi_2O_4$.

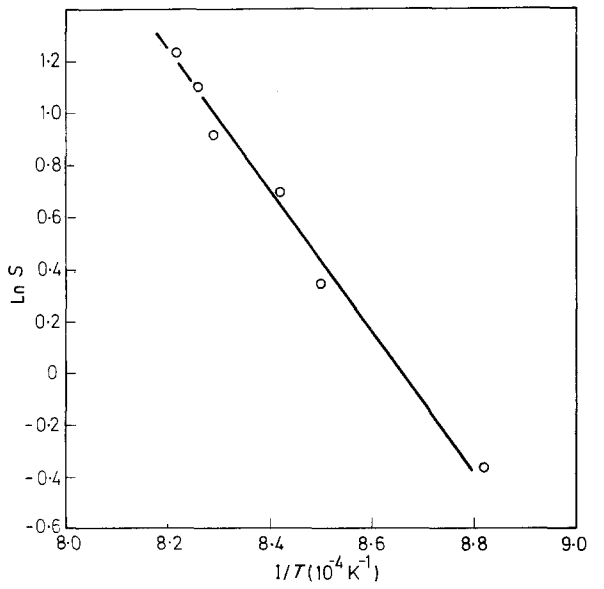

Figure 3 Solubility of CuO in the CuO–$CuBi_2O_4$ system.

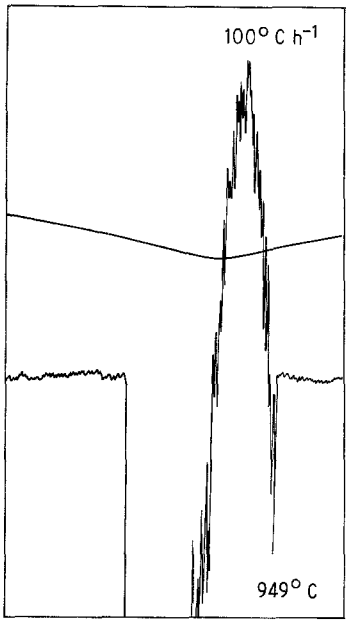

Figure 4 Chart record showing crystallization and dissolution of CuO crystals in the $0.73CuO–0.27Bi_2O_3$ system by ITGA.

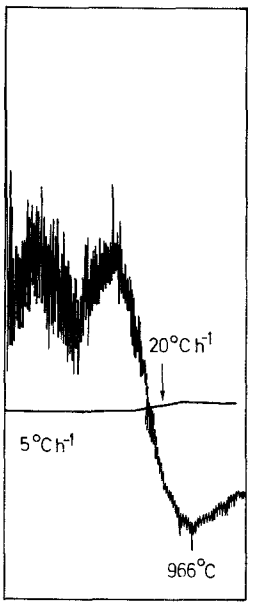

Figure 5 The ITGA curve for a seed crystal in the melt.

dissolved and the TG signal stayed at a constant level with some fluctuation caused by convection. As nucleation started on the platinum wire during cooling, surface tension at the solid–liquid interface led the curve to deviate from the base line. As crystals grew on the wire, the apparent weight rapidly rose, because of the difference in densities between solid and liquid. The fluctuation in weight also became larger. A crystallization temperature of 949 °C was clearly determined for the system $0.73CuO–0.27Bi_2O_3$ under a cooling rate of 100 °C h^{-1}. During successive heatings, the weight decreased as the crystals dissolved, returning finally to the base line.

Fig. 5 shows the ITGA curve of a seed crystal in the solution with the same concentration. Above the crystallization temperature, the apparent weight decreased because of the dissolution of the seed crystal. As the temperature cooled down below the crystallization temperature, the weight increased as the crystal grew in size. The crystallization point of 966 °C, measured with a seed, is higher than the crystallization temperature measured by the immersed platinum wire because of more supercooling in the latter case. The faster the cooling rate, the lower the apparent crystallization temperature. Fig. 6 shows the dependence of crystallization temperature on the cooling rates, which indicates about 20 °C supercooling at high temperature. At a low temperature at the end of crystal growth, supercooling can become larger because of the high viscosity of the system.

3.3. Kinetic analysis of seed dissolution

For the seed-dissolution experiment, a platinum crucible with 150 g mixture of $0.70CuO–0.30Bi_2O_3$ was used. The crystallization temperature was determined by the ITGA–seeding method. Dissolution of a 0.30 g seed crystal was carried out for nearly 2 h at constant temperature with a superheating of about 7 °C and the apparent weight was recorded. Suppose the dissolution process is limited by solute diffusion in the high-temperature solution and there is a diffusion layer with thickness δ on the surface of the crystal. By solving the solute diffusion equation in the stable state [17], we have the rate of dissolution of the seed per unit area of surface

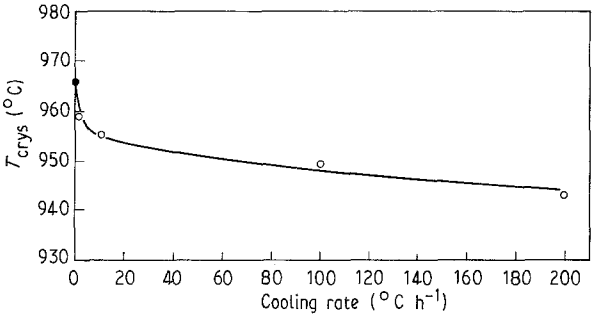

Figure 6 Dependence of crystallization temperature on cooling rates. (●) Value obtained by seeding.

$$V = -(D/\delta)k_2\Delta T/(1 - C_1) \quad (3)$$

in which the diffusion coefficient $D = D_0 \exp(-E/RT)$, E is the diffusion activity energy, k_2 the temperature coefficient of solubility, ΔT the superheating and C_1 the concentration of bulk solution. The dissolution rate is given by

$$\Delta M/\Delta t = -K(T)M^{2/3} \simeq A(T) + B(T)\Delta M \quad (4)$$

where

$$K(T) = k_1 k_2 \rho^{1/3}\Delta T/(1 - C_1)(D_0/\delta)\exp(-E/RT) \quad (5)$$

$$A(T) = -K(T)M_0^{2/3} \quad (6)$$

$$B(T) = 2/3\,K(T)M_0^{2/3} \quad (7)$$

in which k_1 is the surface-to-volume ratio of the seed, ρ the density of the crystal, M_0 the initial weight of the seed and $\Delta M = M_0 - M(t)$ is the loss of the crystal weight during dissolution.

TABLE I Crystal growth of CuO by top-seeding

Experiment	Starting composition			Crucible	Seed position	Slow cooling		Crystals	
	CuO (mol)	Bi_2O_3 (mol)	Weight (g)			Range (°C)	Rate ($°C\,h^{-1}$)	Weight (g)	Size (mm)
1	0.73	0.27	101	Al_2O_3	Near the surface	966–900	1–0.5	13	30 diameter × 4–1 (thickness)
2	0.70	0.30	150	Pt	Near the base	957–900	0.5	20	22 × 20 × 8

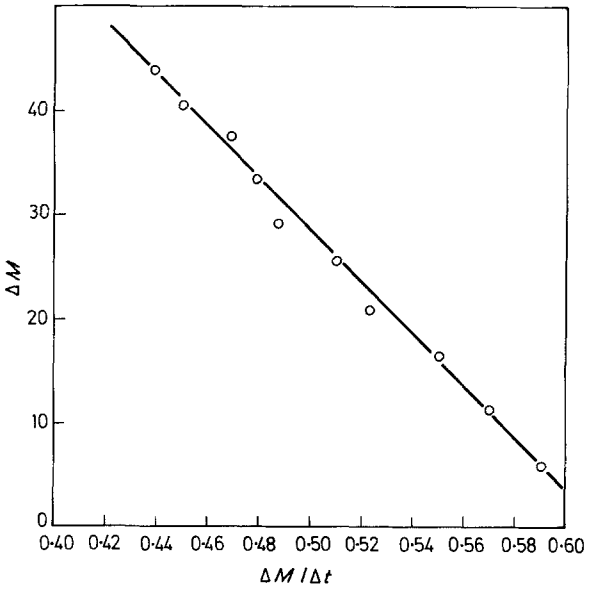

Figure 7 Relative dissolution loss as a function of dissolution rate at constant temperature.

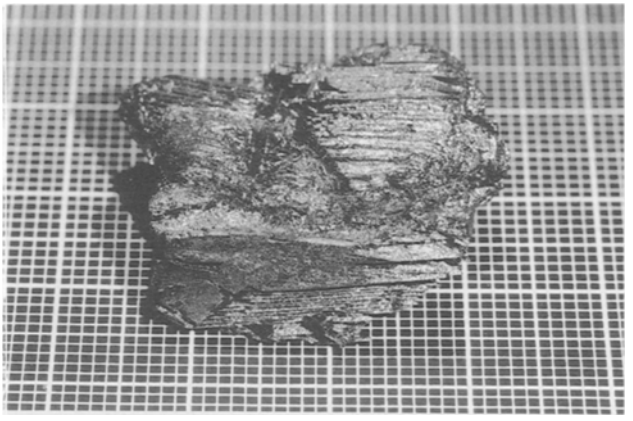

Figure 8 Crystals of CuO grown on the seed.

Fig. 7 shows the relation between $\Delta M/\Delta t$ and ΔM, which indicates that the dissolution rate is linearly dependent on the dissolution loss at a constant temperature or constant superheating under the stable state conditions. As a result, $K(T)$, the function of the temperature, can be obtained from the linear dependence. From Equation 5 we have

$$\ln[K(T)/\Delta T] = C - E/RT \quad (8)$$

$$C = [k_1 \rho^{1/3} k_2/(1 - C_1)]D_0/\delta \quad (9)$$

As a result, a plot of $\ln[K(T)/\Delta T]$ as a function of $1/T$ is still a straight line. From the slope and the intercept, the diffusion activity energy, E, can be determined and the diffusion rate parameter $K_d = D/\delta$ can be calculated. Both are important parameters for crystal growth. In order to grow high quality single crystals, the growth rate must be controlled at a stable state. If the crystal growth rate is also limited by solute diffusion, the stable growth rate has a formula similar to Equation 3 and the effect of different degrees of supercooling can be estimated [17].

3.4. Crystal growth by top-seeding

Using the phase diagram of CuO–$CuBi_2O_4$ (Fig. 2), suitable starting compositions were chosen for crystal growth by top-seeding from alumina or platinum crucibles. After complete dissolution and homogenization at high temperature, the saturation temperature was determined *in situ* by the ITGA–seed method. Crystal growth was then carried out by top-seeding at a slow cooling rate. The crystals could be separated from the flux by hot-pouring above the eutectic temperature. Table I summarizes the experimental conditions and the results of the growth of CuO crystals. Experiment 1 was performed in the spiral SiC tube furnace with temperature gradient of $-4\,°C\,cm^{-1}$ (cooler at the surface than at the bottom). A crystal lid with a shining black surface was grown on the seed near the surface of the solution. Experiment 2 was performed in the three heating-zone furnace with temperature gradient of $1\,°C\,cm^{-1}$ (hotter at the surface than at the bottom). As a result, a crystal block of many crystals, shown in Fig. 8, was grown from the seed near the bottom of the crucible. The saturation temperatures of 966 and 957 °C, which were measured by the seed for the 0.73CuO–0.27Bi_2O_3 and 0.70CuO–0.30Bi_2O_3 systems, respectively, were about 20 °C higher than the crystallization temperature measured by the platinum wire (Fig. 2) at fast cooling rate because of the supercooling. As the temperature decreased, the degree of supercooling became larger.

4. Conclusions

1. The CuO–$CuBi_2O_4$ phase diagram has been established by improved thermogravimetric analysis and by differential thermal analysis.

2. ITGA is very useful not only for determination of the crystallization temperature, but also for kinetic study of crystal dissolution and crystal growth.

3. Large crystals have been grown by ITGA–top seeding from the flux system of CuO–Bi_2O_3.

Acknowledgement

The authors thank the SERC for funding the National Crystal Growth Facility for Superconducting Oxides.

References

1. S. ASBRINK and L. J. NORRBY, *Acta Crystallogr.* **B26** (1970) 8.
2. M. AIN, W. REICHARD, B. HENNION, G. PEPY and B. M. WANKLYN, *Physica C* **162–164** (1989) 1279.
3. R. G. GRAHAM, D. FOWLER, J. S. LORD, P. C. RIEDI and B. M. WANKLYN, *Phys. Rev. B.* **44** (1991) 7091.
4. M. AIN, A. MENELLE, B. M. WANKLYN, G. PARETTE and E. F. BERTAUT, *J. Phys. Condensed Matter* **4** (1992) 5327.
5. A. M. M. GADALLA, W. F. FORD and J. WHITE, *Trans. Brit. Ceram. Soc.* **62** (1963) 57.
6. K-TH. WILKE, *Z. Anorg. Allg. Chem.* **330** (1964) 164.
7. B. M. WANKLYN, F. R. WONDRE and W. DAVISON, *J. Mater. Sci.* **11** (1976) 1607.
8. B. M. WANKLYN and B. J. GARRARD, *ibid.* **2** (1983) 285.
9. CHEN CHANGKANG, HU YONGLE, B. M. WANKLYN and J. M. HODBY, *J. Crystal Growth* **129** (1993) 239.
10. J. CASSEDANNE and C. P. CAMPELO, *An. Acad. Brasil. Cienc.* **38** (1966) 36.
11. CHEN CHANGKANG, B. M. WANKLYN, E. DIEGUEZ, A. J. COOK, J. W. HODBY, A. DABKOWSKI and H. DABKOWSKA, *J. Crystal Growth* **118** (1992) 101.
12. CHEN CHANGKANG and B. M. WANKLYN, *ibid.* **96** (1989) 547.
13. B. M. WANKLYN, CHEN CHANGKANG, J. W. HODBY and C. J. SALTER, *J. Less-Common Metals* **164, 165** (1990) 926.
14. CHEN CHANGKANG and B. M. WANKLYN, *Supercond. Sci. Technol.* **3** (1990) 540.
15. CHEN CHANGKANG, B. E. WATTS, B. M. WANKLYN, P. A. THOMAS and P. W. HAYCOCK, *J. Crystal Growth* **91** (1988) 659.
16. CHEN CHANGKANG, B. M. WANKLYN, D. T. SMITH and F. R. WONDRE, *J. Mater. Sci.* **26** (1991) 5323.
17. CHEN CHANGKANG, *J. Crystal Growth* **89** (1988) 295.

Received 28 July
and accepted 2 September 1992